JOURNAL OF SYNCHROTRON RADIATION
ISSN 1600-5775

Picosecond-resolved X-ray absorption spectroscopy at low signal contrast using a hard X-ray streak camera

Bernhard W. Adams,[a]* Christoph Rose-Petruck[b] and Yishuo Jiao[b]

[a]Argonne National Laboratory, 9700 South Cass Avenue, Argonne, IL 60439, USA, and [b]Brown University, Providence, RI 02912, USA. *Correspondence e-mail: adams@aps.anl.gov

Received 23 November 2014
Accepted 21 April 2015

Edited by S. M. Heald, Argonne National Laboratory, USA

Keywords: X-ray streak camera; high repetition rate; ultrafast laser; photochemistry.

A picosecond-resolving hard-X-ray streak camera has been in operation for several years at Sector 7 of the Advanced Photon Source (APS). Several upgrades have been implemented over the past few years to optimize integration into the beamline, reduce the timing jitter, and improve the signal-to-noise ratio. These include the development of X-ray optics for focusing the X-rays into the sample and the entrance slit of the streak camera, and measures to minimize the amount of laser light needed to generate the deflection-voltage ramp. For the latter, the photoconductive switch generating the deflection ramp was replaced with microwave power electronics. With these, the streak camera operates routinely at 88 MHz repetition rate, thus making it compatible with all of the APS fill patterns including use of all the X-rays in the 324-bunch mode. Sample data are shown to demonstrate the performance.

1. Introduction

When studying the electronic and structural dynamics of chemical or condensed-matter samples, a technique is often used where the sample is photoexcited by a short 'pump' laser pulse and probed by another laser or an X-ray pulse. This ultrafast technique is common in several research fields including photo-induced phase transition in crystals (Cavalleri *et al.*, 2001; Collet *et al.*, 2003), photodissociation (Chen *et al.*, 2001), ligand substitution (Ahr *et al.*, 2011) and photo-biological processes (Tomita *et al.*, 2009). X-rays can provide unique information that is not available in other ways, including changes in the electronic environment of a particular elemental species (oxidation state), changes in the structural coordination of a particular elemental species, or redistribution of the electron density within a molecule or crystal. With this motivation, laser-pump/X-ray-probe experimental techniques have been developed at synchrotron radiation sources. In these, the time resolution is usually limited by the length of the X-ray bunch, typically 50–200 ps. However, a higher time resolution can be achieved by use of a fast detector, such as a streak camera. Several reports describe streak cameras that can achieve sub-picosecond temporal resolution with UV light in accumulating mode (Shakya & Chang, 2005) and with soft X-rays in single-shot mode (Larsson *et al.*, 1997). Such temporal resolution is more difficult to reach in the hard X-ray regime; only recently, a hard X-ray streak camera has achieved a sub-picosecond resolution using the single-photon-counting method.

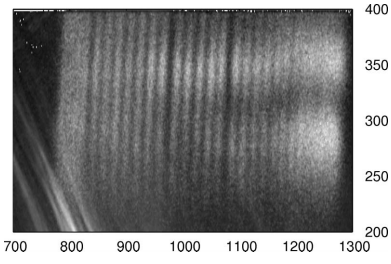

2. Streak cameras

Streak cameras are electron or photon (through conversion to photoelectrons) detectors that are optimized for a high time resolution within a brief time window following the trigger of an event in a sample. Most often, this trigger is provided by a laser pulse. At the core of each streak camera is an electron-optical system that images from an entrance slit to an at least one-dimensionally (often two-dimensionally) resolving electron detector, such as a phosphor screen, or an in-vacuum semiconductor chip. Integrated into these optics is an electric field transverse-deflection unit. Application of a rapid voltage ramp streaks the electron-beam image on the detector, thus mapping time to a spatial coordinate. The deflection unit may consist of a pair of parallel metal plates, or controlled-impedance striplines that are laid out in a meandering pattern to match the average pulse-propagation speed to that of the electrons traversing the deflection unit. For a picosecond resolution, the voltage ramp has to have a rise time of the order of 100 ps at a typical amplitude of 50 to 200 V. This is often achieved by use of a laser-triggered photoconductive switch, *i.e.* a piece of semiconductor material that is suddenly turned conductive by massive charge-carrier generation from a laser pulse split off from the beam triggering the sample. With recent advances in high-power solid-state microwave technology, it is now also possible to achieve the same by using off-the-shelf microwave amplifiers, which are fed a signal from a photodiode triggered by the laser. This approach has the advantage of requiring only a minimal amount of laser power to operate.

3. The streak camera at the APS

A streak camera based on a design by Zhenghu Chang (Chang *et al.*, 1996) has been in operation for several years at Sector 7 of the Advanced Photon Source (APS). It has been described earlier (Chollet *et al.*, 2011), and obtained time-resolved data have been presented (Ahr *et al.*, 2011). Driven by operational experience, especially with respect to X-ray absorption spectroscopy with very low signal contrast, several improvements were implemented over the past three to four years. These include the design of X-ray optics optimized for streak-camera operation (Adams & Rose-Petruck, 2015), replacing the photoconductive switch used for the generation of the deflection voltages with laser-triggered microwave electronics, and replacing the microchannel-plate-amplified phosphor screen with an in-vacuum CCD camera directly exposed to the electron current. These are discussed in detail in the following sections. Fig. 1 shows a schematic view of the streak camera in its current configuration.

3.1. X-ray optics

The X-ray streak camera and the experiments performed with it have some specific requirements of the beamline. First, to focusing: in order to excite a significant fraction of sample molecules, photochemical experiments typically require a high power density of laser light converted to shorter wavelengths

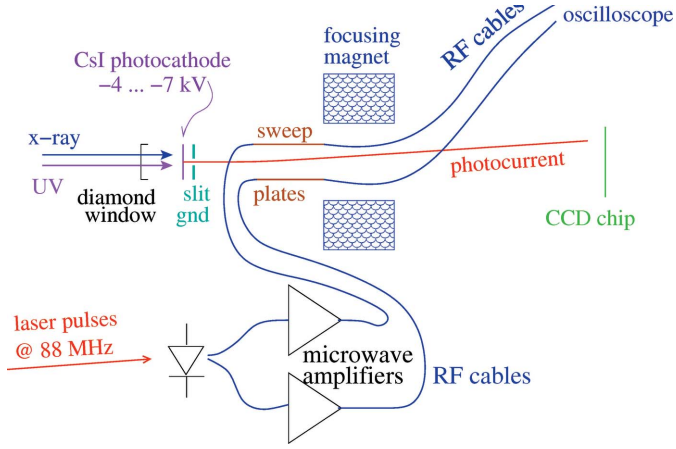

Figure 1
Schematic of the APS streak camera in its current configuration.

than the 800 nm delivered directly by the laser. Due to limited conversion efficiencies, it is then necessary to focus the laser to a tight spot of, typically, less than 100 µm diameter. For a uniform effect of the laser excitation on X-ray spectra, the X-rays must be focused even tighter to about 30 µm. The X-rays must also be focused into the entrance slit of the streak camera, which, in the case of the APS streak camera, is 25 µm high by 3 mm wide, and is situated about 75 cm downstream of the sample. Such a longitudinally extended focus requires an optic with a long focal length, at least regarding focusing in the vertical direction, *i.e.* the smaller dimension of the entrance slit. Of the commonly used focusing elements, *i.e.* lenses, mirrors and Fresnel zone plates, the first appears by far the most attractive: zone plates are designed for close focusing, and none with a long focal length are commercially available. Mirrors deflect the beam by a few tenths of a degree, *i.e.* far away from the beam path over the long focal length. It would take a pair of mirrors to keep the beam on-axis, making this an expensive and complex piece of equipment. That leaves lenses, which leave the X-rays on-axis, and which are also relatively inexpensive due to their small sizes and comparatively relaxed requirements of surface quality. However, a problem with lenses (as well as with zone plates) is their chromatic dispersion. Therefore, the focal length must be adjusted for each X-ray wavelength used, and, in the case of energy scans over more than about 100 eV, the adjustment has to be made during the scan. Various solutions have been tested, such as the use of a wedge-shaped lens body (Khounsary *et al.*, 2002) or a transfocator (Vaughan *et al.*, 2011; Zozulya *et al.*, 2012), which both permit a choice of the number of component lenses to adjust the total focusing power. However, with a long focal length, the number of component lenses is too small to permit a sufficiently fine adjustment in terms of integer steps. Therefore, a method was developed (Adams & Chollet, 2013; Adams & Rose-Petruck, 2015) to continuously vary the effective number of component lenses in a cylindrical lens. Briefly put, the method is based on a rotation about an angle χ in the axis that is perpendicular to the X-rays and the cylinder axis, which introduces a scaling factor $1/\cos\chi$ in the amount of lens material in the beam (see Fig. 2).

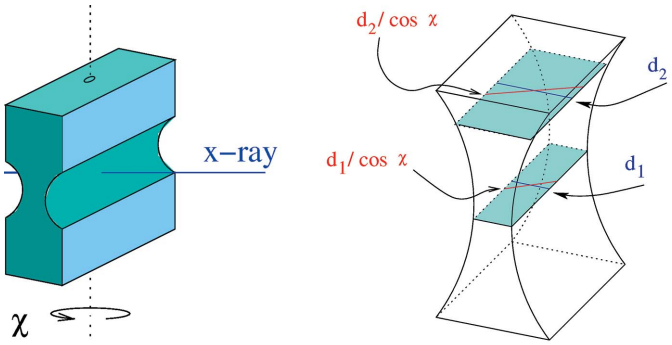

Figure 2
Left: schematic view of a wall between two holes in a cylindrical X-ray lens and the rotation to continuously change the focusing power. Right: two planes in that wall at different distances from the lens center. The rotation introduces the same scaling factor in the amount of material traversed by the X-rays, and thus the same change in the phase advance leading to focusing. See Adams & Chollet (2013) and Adams & Rose-Petruck (2015) for details.

The lens used here consists of a block of Be metal with two cylindrical holes of diameter 1 mm drilled into it. It is placed in the 7-ID-B hutch of the APS at a distance 16 m upstream of the sample and streak camera in the experimental hutch. With this adjustable lens, the vertical focus can be optimized for the sample location and can be maintained there in scans of the X-ray photon energy.

Regarding the horizontal direction, a focus needs to lie only in the sample location, but not on the streak-camera entrance slit, which is wide enough to admit X-rays diverging out of the sample focus. In fact, some spreading of the X-rays over the width of the slit is helpful to avoid rapid radiation degradation of the illuminated spot on the photocathode. Therefore, a much shorter focal length is feasible and desirable for the horizontal direction. A sagittal mirror was chosen for this task. It is placed 1.2 m upstream of the sample, which is well within the extended vertical focus from the long-focusing lens. The footprint of the vertically focused beam on the mirror is rather small (about 16 mm for a 35 µm-high beam at an incidence angle of 0.12°), and thus a relatively inexpensive mirror can be used. The mirror has a cylindrical surface with a radius of curvature of 4 mm. That mirror also serves to suppress the third and higher harmonics of the photon energy nominally selected by the beamline monochromator.

Next, to the X-ray chopper. Because the repetition rate of the X-rays from the APS is much higher than that of the laser (MHz *versus* kHz), most of the X-ray flux does not serve any purpose in the experiment. In order to minimize X-ray degradation of the sample and the photocathode, an X-ray chopper is used that opens for 2 µs every 200 µs. In the hybrid-singlet mode of the APS, this will isolate a single high-current pulse at a rate of 5 kHz, and, in the 24-bunch mode, about 15 bunches are transmitted. Fig. 3 shows an overview of the optics layout.

As in any laser-pump/X-ray-probe experiment, the laser has to be brought into spatial and timing overlap with the X-rays. In the liquid-phase absorption-spectroscopy setup developed for the APS streak camera, spatial overlap is achieved by observing the laser and X-ray foci in two places separated by about 20 mm in the direction along the X-ray beam, using a CCD camera coupled to a microscope lens. The laser is then steered iteratively with two mirrors until it is co-linear with the X-rays (the last laser turning mirror being on a beryllium substrate). Coarse timing synchronization on the level of 30 ps is carried out using an InGaAs photodiode (Teledyne Judson Technologies type No. J22-18I-R40U; Teledyne Judson Technologies, 2004) inside the sample chamber that can be moved into the X-ray and laser beams. This measurement is then refined using the streak camera itself. To that purpose, an optical mirror on a beryllium substrate, which is normally present on the downstream end of the sample chamber, is removed. Then, the UV light that would photoexcite the sample in a measurement reaches the photocathode through the diamond entrance window of the streak camera. The UV pulse will then appear in some location along the streak, depending on the picosecond-level timing of it relative to the deflection (see §3.3).

3.2. Laser optics

The beamline laser is situated in a separate room at the end of the beamline, about 20 m from the streak camera in the experimental hutch. It consists of a Ti:sapphire laser oscillator of type Coherent Mira that has its 88 MHz repetition rate phase-locked to the master clock of the APS, and a regenerative amplifier of type Coherent Legend pumped by a Coherent Evolution laser. Placement in a separate room facilitates stable operation of the laser, but poses some problems with respect to transport of the laser beam because any small wavefront distortions, especially near the laser, will lead to strong spatial-mode fluctuations at the experiment. These effects can be exacerbated by nonlinear-optical effects due to the high pulse intensities. A number of measures were taken to minimize the wavefront distortions, including beam transport through an evacuated beampipe over most of the distance, expansion of the beam cross section, and, instead of using the pulse compressor integrated into the laser amplifier, performing the temporal pulse compression at the end of the transport line. However, even so, the laser beam has to travel through several meters of air inside the laser amplifier and

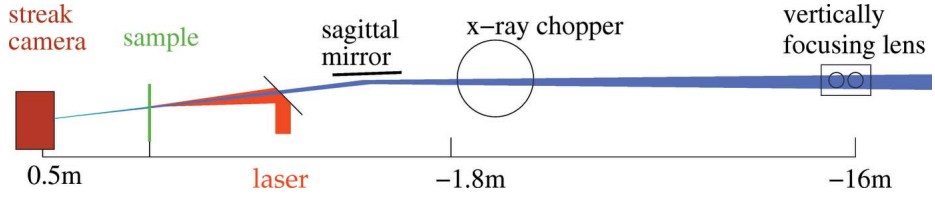

Figure 3
Overview of the optics layout with a cylindrical lens for a long vertical focus, a sagittal mirror for a shorter horizontal focus, an X-ray chopper, co-linear focusing of X-rays and laser onto the sample, and, finally, the streak camera.

through some conditioning optics before it can enter the vacuum. Furthermore, the cavity of the laser amplifier is not specified for strictly single-transverse-mode operation, and apparently some of the spatial-mode fluctuations originate from there. These residual effects were mitigated by installing a relay-imaging optic that reproduces the near-field conditions at the laser exit in the experimental hutch.

3.3. Deflection

The rapid deflection for the picosecond time resolution is achieved by applying a voltage ramp to a set of deflection, or sweep, plates situated about half way between the entrance slit and the magnetic lens (see Fig. 1). These are not just simple metal plates of the kind used in an analog oscilloscope. Rather, they are made of printed-circuit-board material, and have a meandering 50 Ω stripline printed on them. Electric pulses traveling along that stripline then have an average forward velocity of 16% of the speed of light, which is the velocity of the 5 keV electrons in the electron optics. A schematic drawing of such a plate is shown in Fig. 4.

In the original design, the voltage ramp was generated with a photoconductive switch driven by about 30% of the laser pulse energy of 2.5 mJ. This large amount of laser pulse energy was necessary to saturate the switch, and thus reduce the jitter due to fluctuations in the laser-pulse energy. However, even at this large saturation level, a jitter of up to about 10 ps remained, which was apparently caused by variable current paths across the switch due to the spatial-mode fluctuations in the laser beam that are described in §3.2. To operate the streak camera under these conditions, an alternate scheme for generating the deflection voltages was developed that is based on microwave power electronics instead of the photoconductive switch. Even though the laser-transport issues are now largely resolved, that scheme is being retained because it leaves the full laser power for the experiment and can operate at any repetition rate, not just the 1 kHz rate of the amplified laser. In this alternate scheme, a 10% sample of the laser-oscillator beam is sent from the laser room to the experimental hutch alongside the main laser beam, while the other 90% goes to the amplifier, as usual (see Fig. 5). Operational experience shows that the streak camera runs in the most stable way with the deflection voltages derived from the oscillator beam, compared with either the photoconductive switch (which also takes away a large part of the laser power), or the photodiode picking up stray light from the main laser pulse.

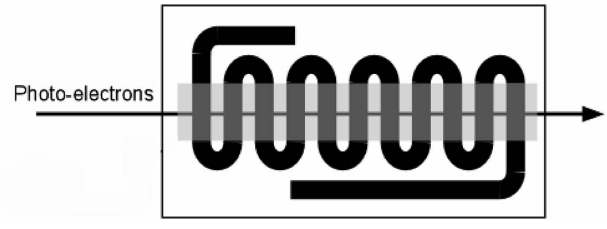

Figure 4
The meandering 50 Ω stripline pattern on a deflection plate.

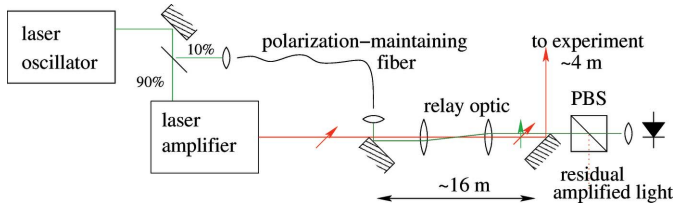

Figure 5
Transport of a 10% sample of the laser-oscillator beam (green) alongside the main amplified laser beam (red). In addition to the geometric separation, a polarizing beamsplitter (PBS) suppresses the main laser signal on the photodiode.

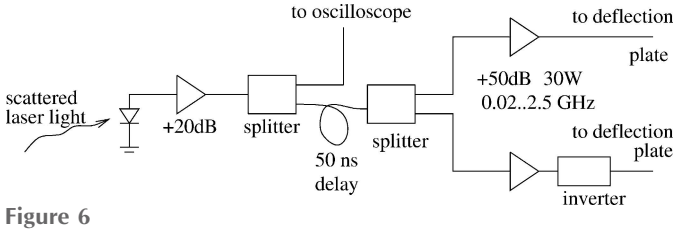

Figure 6
Schematic of the microwave circuitry from the photodiode to the power amplifiers.

The 10% sample is picked up with a thin-plate polarizing beamsplitter that does not significantly broaden the oscillator pulses before they enter the amplifier. It is focused into a polarization-maintaining fiber, and is launched into the vacuum beam-transport tube parallel to the main laser beam, and at a crossed polarization to it. After spatial filtering and suppression of the main laser light with a polarizer, it is focused onto an InGaAs photodiode (Teledyne Judson Technologies type No. J22-18I-R40U) with an active area of 40 µm diameter and about 50 ps rise time. The fiber does broaden the laser pulses, but less so than the photodiode can resolve. Under normal operating conditions, that oscillator beam does not show any discernible spatial-mode or power fluctuations. It is therefore ideally suited for the generation of a low-jitter deflection voltage.[1] The signal from the photodiode is amplified in a chain of microwave amplifiers ending in a pair of 30 W broadband (20 MHz to 2.5 GHz) power amplifiers (RF Lambda model RAPA0M3GW50) that drive the deflection plates, as shown in Fig. 6.

Although the deflection signal consists only of short pulses with a low average power, the high-power amplifiers are needed to drive a sufficient amplitude of 25 V peak into a 50 Ω cable. Initial worries that the power dissipation from the high repetition rate of the deflection signal would result in outgassing and degradation of the vacuum in the electron optics turned out to be unfounded. The relatively low deflection voltages of ±25 V are sufficient for operation with 5 keV electrons from the photocathode and the in-vacuum directly electron-exposed CCD camera described in §3.5. A higher deflection amplitude would yield a longer streak, but

[1] Under certain conditions, however, the oscillator can enter an operational regime where two longitudinal modes beat against each other, resulting in a modulation of the output power at a frequency of the order of 100 kHz to 1 MHz, and with up to 10% amplitude. When not in this regime, the oscillator is very stable.

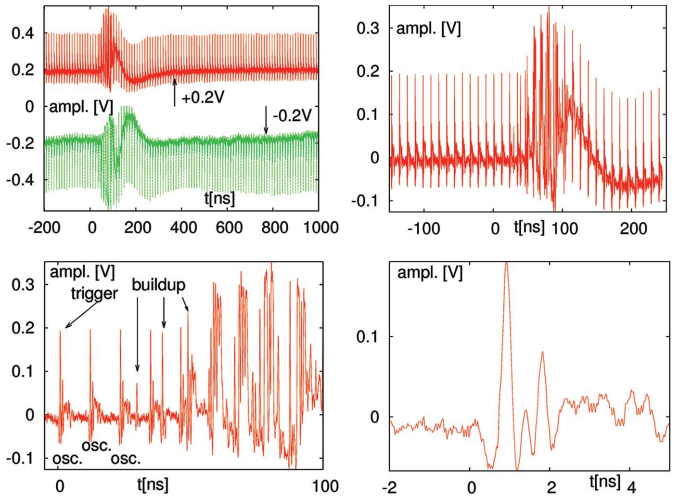

Figure 7
Upper left: both deflection voltages after the attenuators (offset ±0.2 V for graphical clarity). A voltage of 0.2 V after 40 dB power attenuation corresponds to 20 V on the deflection plate. The other three panels show successively more detail.

the image would be degraded proportionally by the electron travel-time dispersion, and no net gain in time resolution would be achieved. The high-repetition-rate operation also permits use of the streak camera in experiments that require a weak excitation at high repetition rate using the laser oscillator alone.

After traversing the deflection plates, the signals continue in 50 Ω coaxial lines to a pair of 40 dB, 50 W attenuators whose outputs go to the oscilloscope for monitoring purposes. Fig. 7 shows oscilloscope traces of the deflection signals after the attenuators.

Despite the spatial filtering and the polarization suppression shown in Fig. 5, some residual light from the main laser beam still reaches the photodiode. The traces thus show a steady sequence of pulses at a repetition rate of 88 MHz, as well as the build-up of the amplified pulse, and the disturbed waveforms after it. The build-up of the amplified pulse is emphasized in the waveform because it is due to leakage from the amplifier cavity while the Pockels cell is still 'shut' and therefore comes at a different polarization from the main pulse. The trace shows that it is important to use one of the undisturbed oscillator pulses before the main one, which is made possible by about 50 ns worth of cable delay, as shown in Fig. 6.

3.4. Timing considerations

One might consider deriving the microwave signal from the APS master clock instead of a photodiode, as was described by Chollet *et al.* (2011). However, the timing relationship between the laser and the APS RF is long-term stable to only about 20 ps, which is sufficient for regular laser-pump/X-ray-probe experiments with 50 to 100 ps time resolution, but not for the streak camera. In contrast to this, the timing relationship between the laser-oscillator pulses driving the deflection and the amplified laser pulses pumping the sample

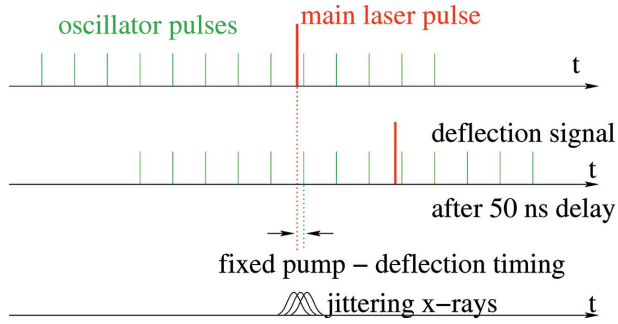

Figure 8
Timing of deflection, sample pump and 'illumination' by the X-rays.

is defined only by optical paths and is stable to better than 1 ps. It does not matter if the X-ray arrival times drift relative to the laser pulses. All this will do is to change the 'illumination' of a fixed event sequence (laser on the sample and deflection in the streak camera). This is shown schematically in the timing diagram of Fig. 8. Fig. 9 shows a schematic of the components relevant to the timing.

The laser oscillator is phase-locked, through an adjustable phase shifter, to the APS master radiofrequency clock. The amplified laser beam reflects this timing because there is a fixed optical path in the amplifier. The deflection in the streak camera is derived from the oscillator timing. The amplified laser beam going to the sample is routed through an optical delay with a retroreflector on a translation stage. It is used to adjust the laser arrival time at the sample, independently of the electronic phase shift. The procedure for obtaining temporal overlap is then to adjust the electronic phase shift so that the deflection voltage derived from the oscillator pulses yields a well streaked image of the X-ray pulses. The amplified laser beam arriving in the experimental hutch has a fixed timing relative to the oscillator pulses, which is determined by the optical paths. Before this amplified laser light is converted from infrared (IR) to ultraviolet (UV), it is sent through an optical delay (a retroreflector on a translation stage). The delay is then adjusted for timing overlap between X-rays and UV laser pulses at the sample location, measured to the 30 ps level with a photodiode. The UV light continues into the streak camera. There, the displacement of the image of the

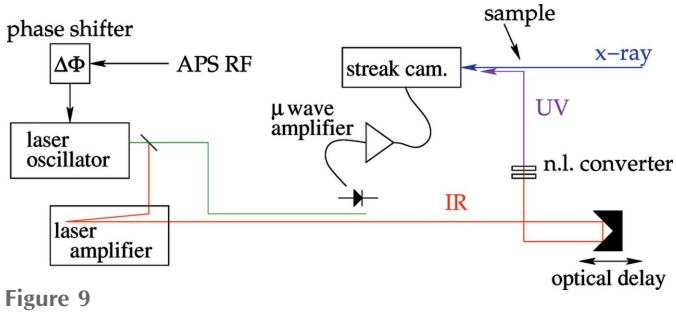

Figure 9
Components of the timing adjustment. The master laser timing is determined by the APS radiofrequency reference with an adjustable phase shift. This affects the oscillator and amplifier beams in the the same way. Additionally, an optical delay varies the laser arrival time at the sample.

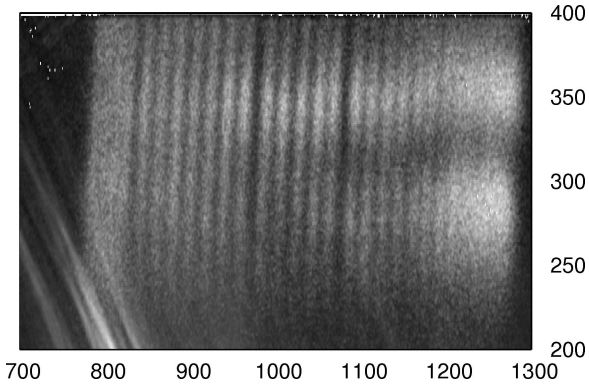

Figure 10
Composite image of UV pulses on the streak camera in 6 ps increments (1 mm steps of the optical delay). The coordinates represent the pixels of the CCD camera.

UV light along the streak indicates the picosecond timing relative to the X-rays. Because UV light and X-rays travel co-linearly from the sample to the streak camera, this relative timing is then the same at the sample (except for minor refractive-index corrections for the UV light as it travels through about 40 cm of air and a 100 µm-thick diamond window). The UV pulse timing is then scanned with the optical delay stage to calibrate the time axis along the streak. Fig. 10 shows a composite image of the UV light pulse in 6 ps increments (1 mm steps of the retroreflecting delay stage).

3.5. Readout

In the original design, the streaked-out electrons hit a pair of microchannel plates (MCPs) that provided an amplified image on a phosphor screen to be recorded with an external CCD camera. The MCPs were also used to gate out unwanted signals, such as those from X-ray bunches not coincident with the laser but admitted by the 2 µs time window of the X-ray chopper. A problem with the use of MCPs is that they introduce a large amount of image noise due to gain inhomogeneities across the field of view and the statistics of the gain process. Solution-phase X-ray absorption spectroscopy measurements (Ahr *et al.*, 2011) typically yield a very low signal contrast of less than 1%, and thus benefit from noise reduction. Therefore, the MCPs were removed, and after trying direct MCP-less observation of the phosphor with a liquid-nitrogen-cooled CCD camera, the phosphor was replaced with an in-vacuum back-illuminated CCD camera that is exposed directly to the electrons (Princeton Instruments model Pixis 400B). With this mode of operation, the streak camera can now detect 0.1% transmission changes with data acquisition times of a few minutes. An example is shown in §4. Image acquisition with the CCD camera is controlled directly from the EPICS beamline software.

Because the MCPs are no longer available for gating out unwanted X-rays, this is now done with a secondary deflection unit that sends unwanted electrons onto a grounded metal plane.

3.6. Secondary deflection

The main deflection unit that provides the rapid streak is situated about half way between the entrance slit and the magnetic lens (see Fig. 1). In addition to that, two types of secondary deflection mechanisms are installed about 20 cm after the lens. One is a pair of Helmholtz coils outside of the vacuum tube to provide magnetic deflection. The other is a set of four electrostatic deflection plates rotated by 45° to match the image rotation induced by the lens.

The Helmholtz coils deflect the electrons in a direction orthogonal to the streak direction in the rotated image. They are used for providing reference streaks as described below. The secondary electrostatic deflection unit is used both as a static bias for centering the streak image on the CCD chip and for gating image acquisition. Two of the plates that are effective in the direction along the streak, and one for the transverse direction, are used for static biasing at voltages between 100 and 200 V. With 800–1000 V applied to the fourth plate, the streak image is shifted away from the CCD chip and onto the ground plane surrounding it. The image from the X-rays that are coincident with the laser is then gated in by taking that voltage to 0 V for 120 ns, *i.e.* less than the bunch spacing in the 24-bunch mode of the APS. By gating in at 0 V, the scheme becomes insensitive to fluctuations in the high voltage applied to the pulser, which may occur due to the pulsed load that the pulser presents to the high-voltage power supply.

Low signal levels of the order of 0.1% can be seen only by taking differences of streaks with and without laser excitation of the sample. When taken successively in two separate exposures, these two images differ in statistical ways caused by subtle fluctuations, such as the thickness of the liquid jet of the sample solution. Furthermore, in this mode, half of the beam time has to be devoted to the reference images. These problems can be avoided by taking the reference almost simultaneously with the laser from otherwise unused X-rays passed by the chopper. The chopper opens up for 2 µm every 200 µs. Only one in five of these openings is actually timed to the 1 kHz laser, and one of the other four can be used for the reference. This is done by switching the current in the Helmholtz coils, as shown in the timing diagram of Fig. 11, to produce two parallel streaks, as shown in the raw image in Fig. 12. The top trace in Fig. 12 is coincident with the laser, and the bottom trace is the reference.

There is a faint pattern in the images which appears to be inherent to the CCD chip. It is visible as faint diagonal stripes in Fig. 12 and can lead to artifacts in the processed data. Furthermore, there are subtly different aberrations in the two streaks that make a direct subtraction of one from the other very difficult. Therefore, the roles of the two streaks are being switched periodically, *i.e.* each exposure is actually taken twice, once with the coincident streak on top and the reference at the bottom, and once with these roles reversed. This results in two data sets that are being processed separately, and that are compared in the end to discriminate real effects from artifacts.

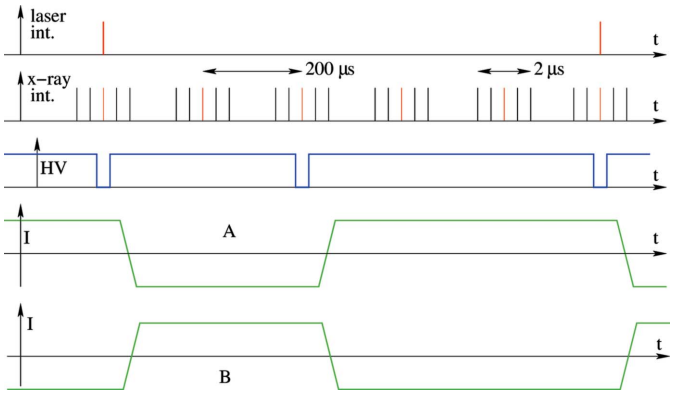

Figure 11
Timing diagram. Top: laser pulses once per millisecond; 2nd: X-rays admitted by the chopper, 2 µs bursts every 200 µs; 3rd: high-voltage gate; 4th and 5th (bottom): the two patterns of current in the Helmholtz coils to put the signal into the top trace and the reference below (*A*), or *vice versa* (*B*).

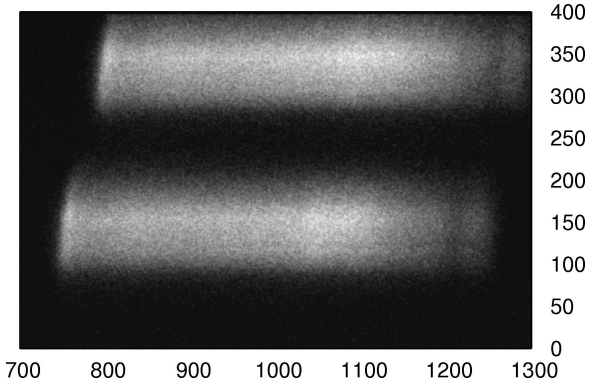

Figure 12
Raw image showing the two parallel streaks. The coordinates represent the pixels of the CCD camera.

Because the APS routinely runs in top-up operation, the relative amounts of charge in the bunches, and thus the intensities from them, change every 2 min. This would make it very difficult to take meaningful differences of streaks due to different bunches. It is therefore important to set the 120 ns high-voltage gate such that the two streaks are produced by the physically same electron bunch of the 24 in the storage ring and among the 10 to 15 pulses admitted by the chopper in its opening interval.

4. Results

The streak camera in the configuration described here has been used for X-ray absorption spectroscopy in transmission mode to measure charge transfer in photoexcitation of aqueous solutions of iron hexacyanoferrate and potassium permanganate. For illustration, Fig. 13 shows a processed data set of the transmission change due to laser excitation through a 1 mmol solution of potassium(III) hexacyanoferrate. These data were taken at several X-ray photon energies near the iron

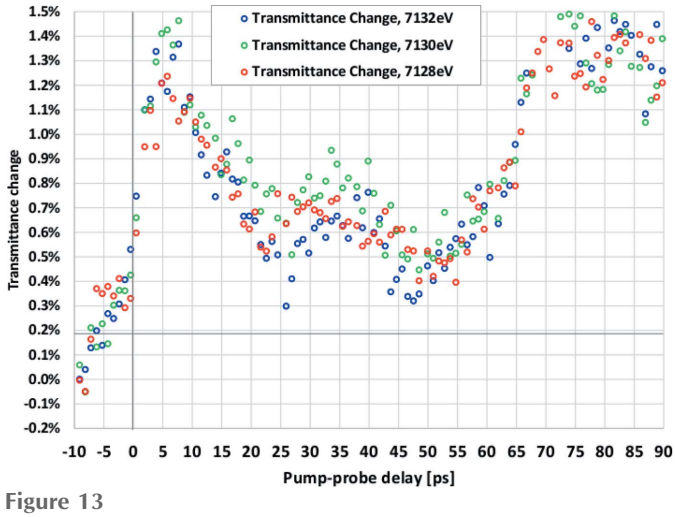

Figure 13
A sample data set showing transmission changes through a 1 mmol solution of potassium(III) hexacyanoferrate due to 266 nm laser excitation.

K-edge, as indicated in the figure. The laser light was frequency-tripled to a wavelength of 266 nm, and the pulse energy was 20 µJ into a 70 µm focus. The transmission change was determined by subtracting the reference streak from that with laser pump, separately for the two configurations (coincident in the upper, reference in the lower trace, and *vice versa*) described in §3.6 and normalizing with the reference streak. The noise is of the order of 0.1%, and there is a clear time dependence of the transmitted X-ray intensity after laser excitation. A detailed discussion of the results will be presented in another publication. Here, we only point out that, immediately following the laser excitation, the transmission increases by about 1% and decays within 10 ps. We attribute this to electronic configuration changes due to the photoexcitation. This is then followed by an oscillation with a period of 10 ps, and another 1% increase in transmission. These latter changes may be due to local-phonon-mode oscillations in the solvation shell surrounding the excited molecule. This sample data set demonstrates the time resolution and the signal-to-noise performance of the streak camera.

One may note that the baseline before time-zero is not entirely flat. This is likely due to those early times being near the beginning of the visible streak where the errors are larger due to lower intensities (compare the streak images in Fig. 12).

Acknowledgements

This work was supported by the US Department of Energy, Office of Basic Energy Sciences under Contract No. DE-AC02-06CH11357. We would also like to thank Yuelin Li and Haidan Wen of Sector 7 at the APS for their support of laser operations.

References

Adams, B. & Chollet, M. (2013). US Patent 8611502.
Adams, B. W. & Rose-Petruck, C. (2015). *J. Synchrotron Rad.* **22**, 16–22.

Ahr, B., Chollet, M., Adams, B., Lunny, E. M., Laperle, C. M. & Rose-Petruck, C. (2011). *Phys. Chem. Chem. Phys.* **13**, 5590–5599.
Cavalleri, A., Tóth, C., Siders, C., Squier, J., Ráksi, F., Forget, P. & Kieffer, J. (2001). *Phys. Rev. Lett.* **87**, 237401.
Chang, Z., Rundquist, A., Zhou, J., Murnane, M. M., Kapteyn, H. C., Liu, X., Shan, B., Liu, J., Niu, L., Gong, M. & Zhang, X. (1996). *Appl. Phys. Lett.* **69**, 133–135.
Chen, L., Jäger, W., Jennings, G., Gosztola, D., Munkholm, A. & Hessler, J. (2001). *Science*, **292**, 262–264.
Chollet, M., Ahr, B., Walko, D., Rose-Petruck, C. & Adams, B. (2011). *IEEE Select. Top. Quantum Electtron.* **18**, 66–73.
Collet, E., Lemée-Cailleau, M.-H., Cointe, M. B.-L., Cailleau, H., Wulff, M., Luty, T., Koshihara, S., Meyer, M., Toupet, L., Rabiller, P. & Techert, S. (2003). *Science*, **300**, 612–615.
Khounsary, A. M., Shastri, S. D., Mashayekhi, A., Macrander, A. T., Smither, R. K. & Kraft, F. (2002). *Proc. SPIE*, **4783**, 49–54.
Larsson, J., Heimann, P. A., Chang, Z., Judd, E., Bucksbaum, P. H., Kapteyn, H. C., Lee,R. W., Liu, X., Machacek, A., Murnane, M. M., Padmore, H. A., Schuck, P. J., Shan, B., Wark, J. S. & Falcone, R. W. (1997). *Opt. Lett.* **22**, 1012–1014.
Shakya, M. & Chang, Z. (2005). *Appl. Phys. Lett.* **87**, 041103.
Teledyne Judson Technologies (2004). *Indium Gallium Arsenide Detectors.* Teledyne Judson Technologies, Montgomeryville, PA 18936, USA.
Tomita, A., Sato, T., Ichiyanagi, K., Nozawa, S., Ichikawa, H., Chollet, M., Kawai, F., Park, S. Y., Tsuduki, T., Yamato, T., Koshihara, S. & Adachi, S. (2009). *Proc. Nat. Acad. Sci.* **106**, 2612–2616.
Vaughan, G. B. M., Wright, J. P., Bytchkov, A., Rossat, M., Gleyzolle, H., Snigireva, I. & Snigirev, A. (2011). *J. Synchrotron Rad.* **18**, 125–133.
Zozulya, A., Bondarenko, S., Schavkan, A., Westermeier, F., Grübel, G. & Sprung, M. (2012). *Opt. Express*, **20**, 18967–18976.